EXPERIMENTAL INVESTIGATION OF THE EFFECTS OF DIFFERENT HELICOPTER ROTOR TIP GEOMETRIES ON AERODYNAMIC PERFORMANCE AND TIP VORTEX CHARACTERISTICS

Sinem Uluocak,
sinem.uluocak@tai.com.tr
Turkish Aerospace Industries, Ankara, Turkey

Hooman Amiri Hazaveh[2] , Mustafa Perçin[3] , M. Tuğrul Akpolat[4] Oğuz Uzol[5]
Department of Aerospace Engineering, Middle East Technical University, Ankara, Turkey

Abstract
In this study, the effects of different tip geometries (rectangular, anhedral, swept-tapered and swept-tapered-anhedral) on the rotor hover performance and tip vortex characteristics are investigated experimentally. A scaled rotor model set-up, instrumented with thrust and torque sensors, is used for aerodynamic performance measurements in hover and a two-dimensional (2D) particle image velocimetry (PIV) is used to obtain the tip vortex characteristics such as vortex trajectory, maximum tangential velocity, and circulation. Although taper+swept and taper+swept+anhedral configurations have the best C_T/C_Q values at lower blade loadings, at higher blade loadings anhedral case has the best performance and an increase of 0.03 figure of merit compared to the baseline. It is observed that different tip shapes change the vortex trajectory, in addition, reduces maximum tangential velocity and circulation significantly. The PIV measurements which were performed at a high blade loading show that there is a correlation between the aerodynamic performance and the vortex strength.

NOMENCLATURE

a_∞	Speed of sound, m/s
$ANHD$	Anhedral Blade
BVI	Blade Vortex Interaction
c	Chord Length
C_T	Rotor Thrust Coefficient, $C_T = T/(0.5\rho(\Omega R)^2 A)$
C_Q	Rotor Torque Coefficient, $C_Q = Q/(0.5\rho(\Omega R)^2 RA)$
FOM	Figure of Merit, ${C_T}^{3/2}/\sqrt{2}C_Q$
LDV	Laser Doppler Velocimetry
M_{tip}	Tip Mach Number, $\Omega R/a_\infty$
N_b	Number of blades
PIV	Particle Image Velocimetry
R	Rotor Radius, m
r/c	Non-dimensional radial coordinate
r_c	Core radius, m
$RECT$	Rectangular Blade
RPM	Revolutions per minute
$TAPER$	Taper+Swept Configuration
TSA	Taper+Swept+Anhedral
V_{tip}	Rotor Tip Speed, ΩR, m/s
V_θ	Vortex tangential velocity, m/s
$V_{\theta,max}$	Maximum tangential velocity
Γ	Circulation, $=2\pi R V_\theta$,m^2/s
σ	Rotor solidity, $N_b c/\pi R$
φ, ϕ	Wake Age, degree
x/c	Non-dimensional axial coordinate

1. INTRODUCTION

Tip vortex is the rotary air flow structure at the tip region, which occurs due to the pressure difference between the lower and upper surfaces of the wing. For fixed wing aircrafts, tip vortices convect downstream in the wake of the wings, so that they have relatively minor influence on the free-stream flow. Moreover, the decrease of aerodynamic performance due to this three-dimensional flow structure around the wing tips is minimized to some extent by use of winglets. On the other hand, for rotary-wing aircrafts, such as helicopters, tip vortices follow a rotary path and they produce a complex and unsteady flow field around the rotor. That complex flow not only decreases aerodynamic performance but also generates noise as a result of Blade Vortex Interaction (BVI) especially in descending and forward flight configurations. Therefore, different tip geometries are designed and studied to mitigate the effect of tip vortex. Tangler and et al. [1] conducted hotwire anemometry and force/torque measurements in hover configuration

Presented at 44th European Rotorcraft Forum, Delft, The Netherlands, 19-20 September, 2018

and observed that the swept tip shows at least 3 percent performance improvement compared to the square tip at the mid-thrust generation regime. They also found that the tip vortex for the double-swept tip has the lowest tangential velocity and the largest core size. Weller [2] carried on performance tests on blades with rectangular, swept, tapered, anhedral tips and their combinations. It was revealed that the blade tip with anhedral gives the best aerodynamic performance in hover and for low advance ratios. Mullins et al. [3] performed pressure measurements in a transonic wind tunnel with fixed blades and the order of performance from high to low was presented as swept-tapered, swept, rectangular and tapered. They also observed that for the swept and swept-tapered planforms, the tip vortex is diffused more than the others. Different tip shapes were tested with LDV by Martin and Leishman [4] and it was observed that tip sweep decreases both the radial and axial convection of the vortex, while taper increases the radial convection and decrease the axial convection. Han and Leishman [5] designed and tested a new tip shape named as the slotted blade which enables the air pass through the holes inside the blade and goes out at the tip region. Laser Doppler Velocimetry (LDV) measurement results showed that the slotted blade reduced the peak value of the swirl velocity up to 60% relative to the baseline blade with a 3% increase in the required rotor power. After the developments in image recording and processing technology, Particle Image Velocimetry (PIV) technique took the place of other techniques since a complete image of velocity field can be obtained easily and rapidly. In recent years, helicopter vortex characteristics were investigated in detail via PIV to understand the effect of meandering [6], [7], active twist [8] and dynamic stall [9]. In this study, both force-torque, and two-dimensional (2D) PIV measurements are conducted to investigate the effects of different rotor tip geometries. The results are used to explore the relation between the aerodynamic performance and the characteristics of the tip vortex, and to find out the tip shape which gives the best performance for the corresponding rotor configuration.

2. EXPERIMENTAL SETUP

2.1. Rotor Test Setup

In the first phase of this experimental study, an open horizontal axis helicopter rotor test setup was designed and manufactured. Five-bladed rotor with a diameter (2R) of 1300 mm is driven by a 200 kW electric motor which maintains speeds up to 3000 RPM, corresponding to a tip Mach number of 0.6. VR7 airfoil profile is chosen for blades. Torque and RPM measurements are performed by using an HBM T40B contactless torque meter mounted on the rotor shaft. For thrust measurements, the whole system including the engine, the rotor and the shaft is placed on a sliding table. An HBM S9M load cell, connecting the sliding table to the fixed part of the bench is used to measure the thrust (Figure 1). A schematic of the design and the manufactured setup are illustrated in

Figure 2 and Figure 3.

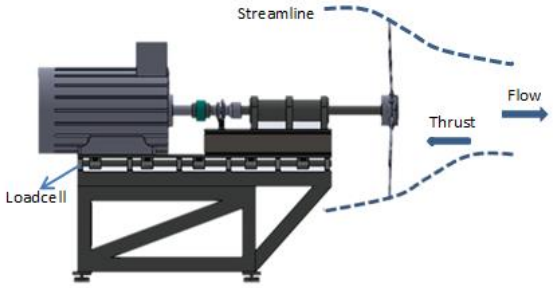

Figure 1: Conceptual wake drawing and loadcell placement

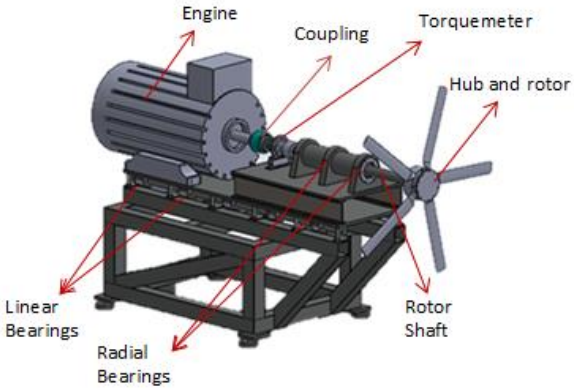

Figure 2: Schematic of the design

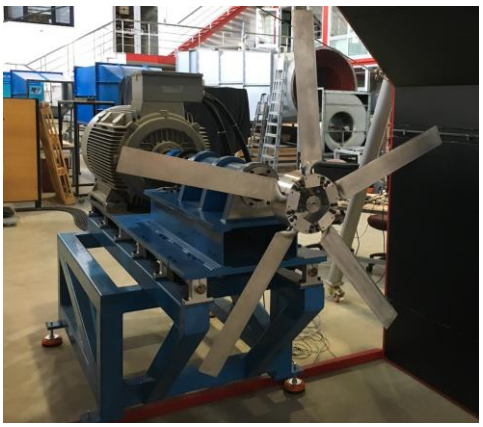

Figure 3: Manufactured setup

Presented at 44th European Rotorcraft Forum, Delft, The Netherlands, 19-20 September, 2018

For this study, tip design modifications were made in the area 0.1 R away from the tip of the blade. Anhedral angle was selected as 15°, sweepback angle was applied as 20° and taper ratio was chosen as 0.6 (Figure 4). Modified blade names were abbreviated as shown in the caption of the Figure 4 and will be presented in this way in the results section.

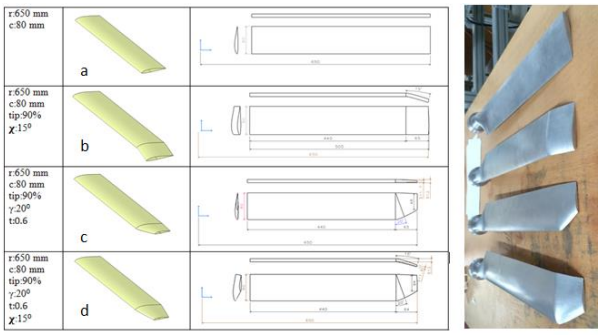

Figure 4: Different Rotor Tip Geometries
a) Rectangular (RECT) b) Anhedral (ANHD)
c) Tapered+Swept (TAPER)
d) Tapered+Swept+Anhedral (TSA)

Test matrix for the thrust and torque measurements is shown in Table 1. Thrust and torque data were taken for a minute at a sampling rate of 2400 Hz after waiting for a minute at the desired RPM value to eliminate any transient effects. For each setting, the thrust and torque measurements were repeated for 5 times to allow for ensemble averaging of the data. The results are presented in the form of non-dimensional thrust and torque coefficients, which are calculated by using thrust, torque, air density and RPM values for each particular measurement. Thrust and torque measurements have less than 0.5% uncertainty with 95% confidence level.

Table 1.Test Matrix for the Thrust and Torque Measurements

Blades	M_{tip}	Pitch Angle
RECT	0.3	5.8°
ANHD	0.4	12°
TAPER		16°
TSA		18°
		20°

2.2. Particle Image Velocimetry

The 2D PIV system consists of an Nd:YAG laser with a wavelength of 532 nm, a maximum repetition rate of 15 kHz, and a pulse energy of 120 mJ/pulse. A fog generator was used to fill the room with particles of 1μm diameter, which were used as tracer particles. Double-frame images of tracer particles were recorded by use of a Phantom v640 camera with a maximum resolution of 2560×1600 pixels^2 and an image recording rate of 1.5 kHz at full resolution. Proper optics (mirrors, spherical and cylindrical lenses) were used to guide the laser beam and convert it to a laser sheet aligned perpendicular to the shooting direction of the camera. Phase-locked measurements were performed using a Hall effect sensor placed on the bench with its magnet attached to the rotor shaft in order to synchronize the rotation of the rotor with the PIV system. This sensor sends one-per-rev signal to the synchronizer box. The laser and the camera can then be triggered at the predetermined azimuthal positions of the rotor by selecting a proper trigger time delay. The time interval between two laser pulses was 15 μs. The experiments were conducted at different azimuthal positions of the rotor between 0° and 72° phase angles (see Figure 5). Phase 0° is defined as the azimuthal position of the rotor for which the laser cuts the quarter-chord of a pre-specified blade at the tip. Phase definitions are shown in Figure 5. Figure 6 shows the test facility while performing the phase-locked PIV measurements at the rotor phase 0°.

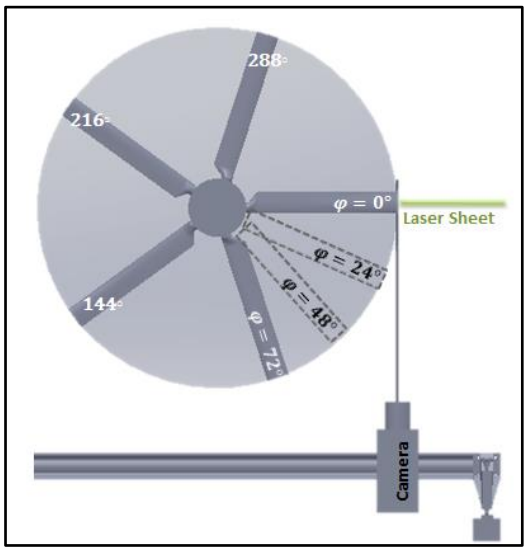

Figure 5: Wake/Phase Age Definitions

The PIV measurements were conducted at the tip Mach number of 0.4 and at the pitch angle of 16° for all of the blades considered in this study. For each phase, 1000 image pairs were recorded. Three tip vortices with a phase difference of 72° (i.e., tip vortices of three subsequent blades) are captured in the field of view, which has dimensions of 288×180 mm^2. Therefore, vortex trajectory and characteristics can be followed in the wake for two blade passages after the formation of the tip vortex.

Presented at 44th European Rotorcraft Forum, Delft, The Netherlands, 19-20 September, 2018

Data acquisition, image pre-processing including the masking of the blade in the images and vector calculation were performed in DANTEC Dynamic Studio. Double-frame particle images were interrogated using interrogation windows of size 64×64 pixels with an overlap factor of 50%. The resultant vector spacing is 3.44 mm in both directions forming a dataset of 79×49 velocity vectors in the measurement plane.

The center of the tip vortex is tracked by use of the γ_1 scheme [10]. As this algorithm is not Galilean invariant, the calculations were performed after subtracting the convection velocity of the particular vortex of interest at each measurement phase. A conditional averaging is then applied on the vector field in a limited neighborhood of the vortex in order to eliminate the effects of vortex meandering and to improve signal-to-noise ratio.

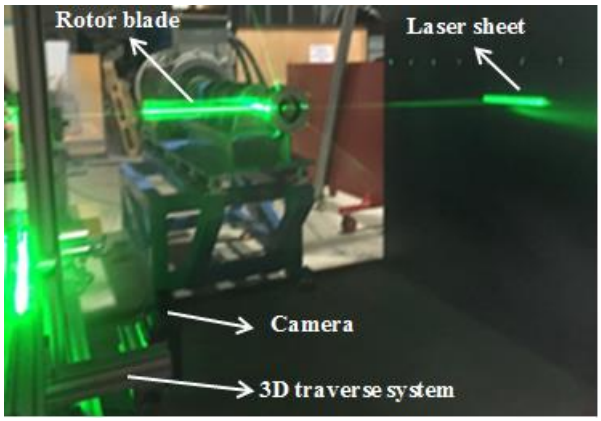

Figure 6: PIV System

3. RESULTS & DISCUSSION

3.1. Performance Results

Aerodynamic performance graphs are presented in terms of coefficients of thrust per torque required, which are normalized by the solidity of the blades. For both Mach numbers, as shown in Figure 7 and Figure 8, the TAPER and the TSA show significant performance increase at relatively low blade loading values, however their effect decreases when the blade loading increases. The performance decrease of the TAPER blade may be attributed to premature stall at the tip region due to the smaller chord length and hence lower Reynolds number [11]. ANHD has the best performance for high blade loadings and it can be compared to the RECT blade in terms of Figure of Merit (FOM) since they have almost the same blade loading. It is clear from Figure 9 that ANHD reaches a maximum FOM value of 0.67 and provides a FOM improvement of approximately 0.03 compared to the RECT blade at M_{tip}=0.3. It is indeed expected to get lower FOM values than the full-scale rotor because of not having both the Reynolds and the Mach numbers similar to the full-scale conditions [12]. The abrupt loss in performance for all geometries at M_{tip}=0.4 originates from a decrease in C_T and it is likely to be a result of the characteristics of the VR7 airfoil at this very Mach Number [13].

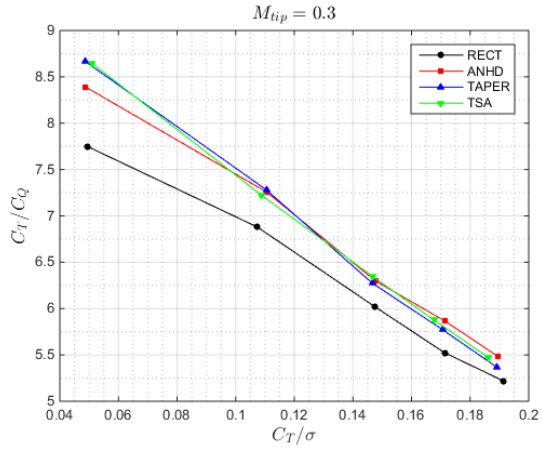

Figure 7: $C_T/\sigma\ vs.\ C_T/\ C_Q\ at\ M_{tip} = 0.3$ for all geometries

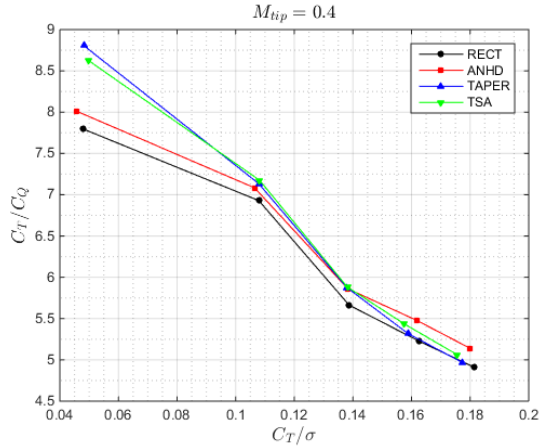

Figure 8: $C_T/\sigma\ vs.\ C_T/\ C_Q\ at\ M_{tip} = 0.4$ for all geometries

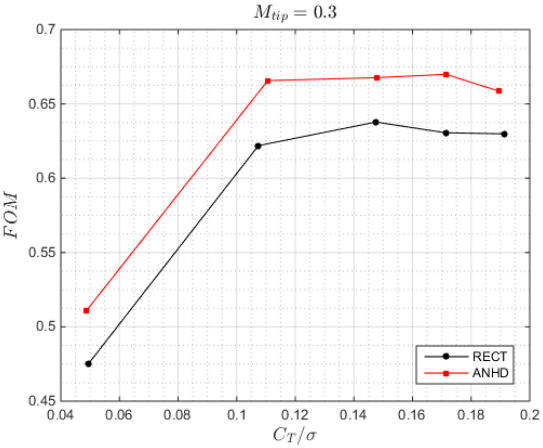

Figure 9: $C_T/\sigma\ vs\ .\ FOM\ at\ M_{tip} = 0.3$

Presented at 44th European Rotorcraft Forum, Delft, The Netherlands, 19-20 September, 2018

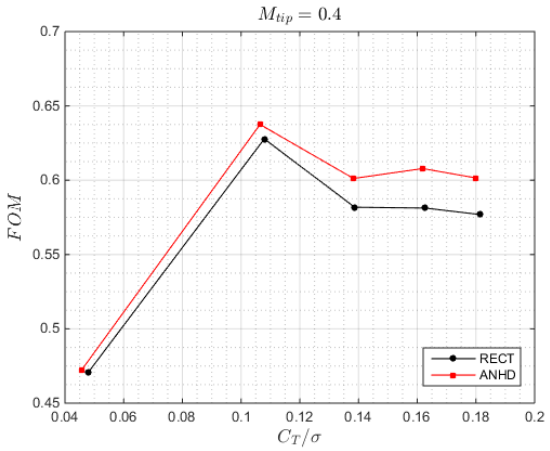

Figure 10: C_T/σ *vs.* FOM *at* $M_{tip} = 0.4$

3.2. PIV Results

Contours of out-of-plane vorticity are shown in Figure 11 for the ensemble -averaged velocity fields corresponding to the phase angles of $\varphi = 0°, 18°, 42°$ and $66°$ for the case of RECT blade. At $\varphi = 0°$, three tip vortices are present in the field of view, i.e. a new tip vortex forming at the tip of the blade and two other vortices that are shed during the last two blade passages. As the blade rotates, the newly formed tip vortex moves radially toward the root of the rotor while it convects downstream. This downward directed motion is more dominant in the immediate wake of the blades, whereas the tip vortices in the relatively far wake convect more in the horizontal direction. Another observation regarding the topology of the vortices is that they display diffused formation rather than a circular shape. This may be attributed to the angle between the measurement plane and the vortex tube as well as the influence of the meandering on the ensemble averaging process. In order to assess this, a conditional averaging is applied on the vector fields and contours of out-of-plane vorticity are plotted for the phase angle of $\varphi = 42°$ for the four different blade tip configurations (Figure 12). It is clear that the aforementioned non-regular shape of the vortices is mostly due to wandering of the vortices. It is also evident from the vorticity plots that in the case of TAPER and TSA configurations, the vorticity levels of the tip vortices decrease considerably. The conditional-averaged velocity vector fields are used for further analysis of the tip vortex behavior, such as vortex trajectories.

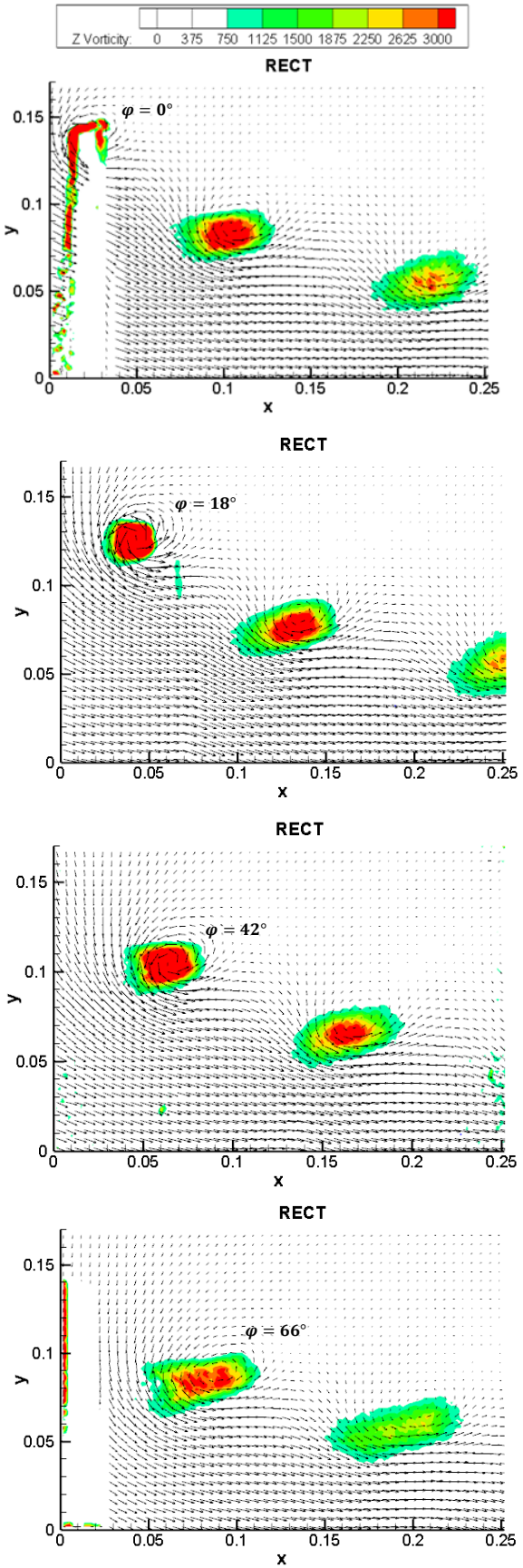

Figure 11: Ensemble-averaged contours of out-of-plane vorticity for $\varphi = 0°, 18°, 42°$ *and* $66°$

Presented at 44th European Rotorcraft Forum, Delft, The Netherlands, 19-20 September, 2018

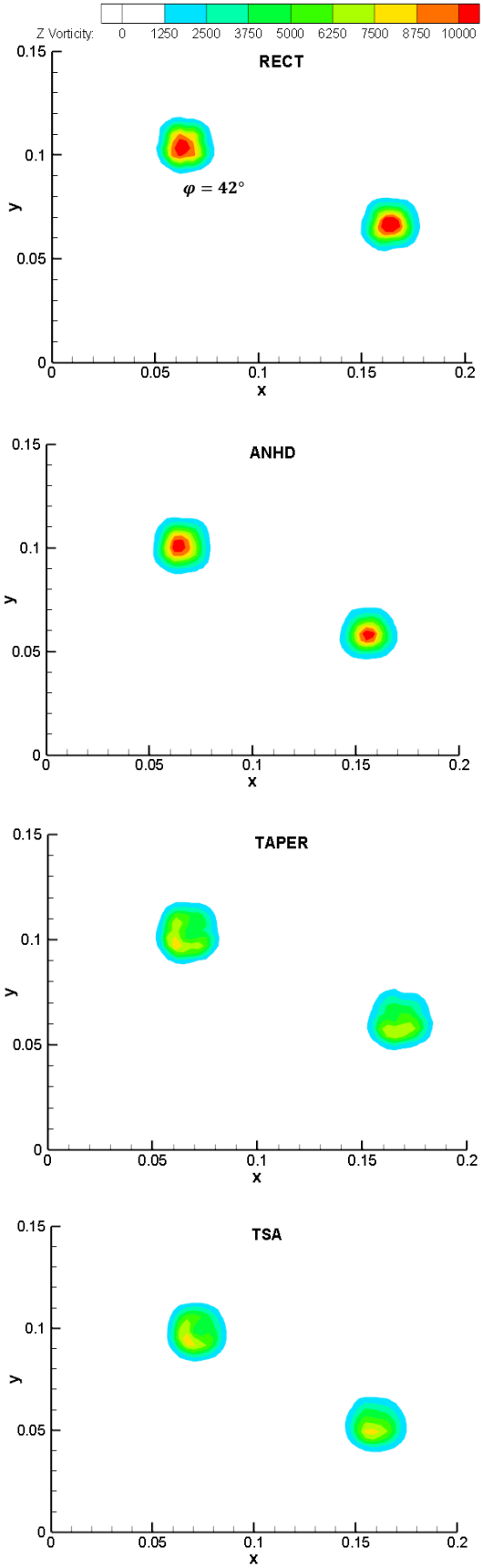

Figure 12: Conditional averaged contours of out-of plane vorticity for $\varphi = 42°$

Different tip geometries significantly alter the wake trajectory. It can be seen from Figure 13 that the tip vortex in the case of ANHD, TSA and TAPER blades convect more radially than that in the case of the rectangular blade. On the contrary, the tip vortex in the case of the RECT blade has a higher axial convection.

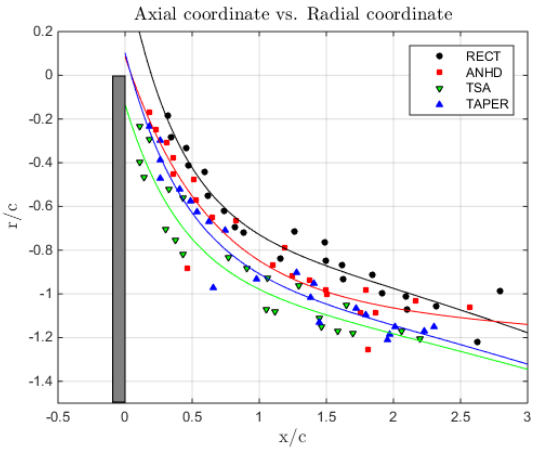

Figure 13: Vortex Trajectory for all Geometries

Velocity profiles passing through the vortex center are obtained from the conditional-averaged velocity fields for the phase range of 18° - 150° for all blades. From Figure 14, which corresponds to $\varphi = 114°$, it can be deduced that the ANHD reduces vortex tangential velocity up to 20%; the TAPER and the TSA reduces it up to 30%. An increase in vortex radius can also be observed for the TAPER and the TSA.

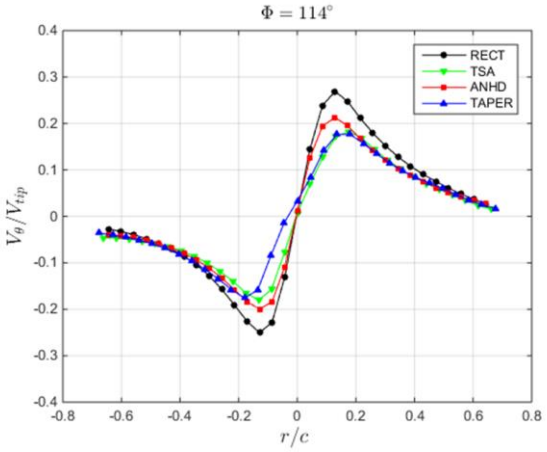

Figure 14: Tangential Velocity Profiles at $\varphi = 114°$

The magnitude of the peak tangential velocity of the tip vortex is an important parameter in terms of vortex sound generation [14]. In this context, phase-history of the maximum tangential velocities of the tip vortices are plotted in Figure 15, which is complemented with a curve fitted by use of a linear regression. As expected, $V_{\theta,max}$ is

Presented at 44th European Rotorcraft Forum, Delft, The Netherlands, 19-20 September, 2018

decreasing with wake age due to the diffusion of the tip vortex. The highest velocity occurs in the case of the RECT blade. It is obvious that all of the tip modifications result in a decrease in the magnitude of the peak tangential velocity and the minimum $V_{\theta,max}$ is achieved in the case of the TSA blade.

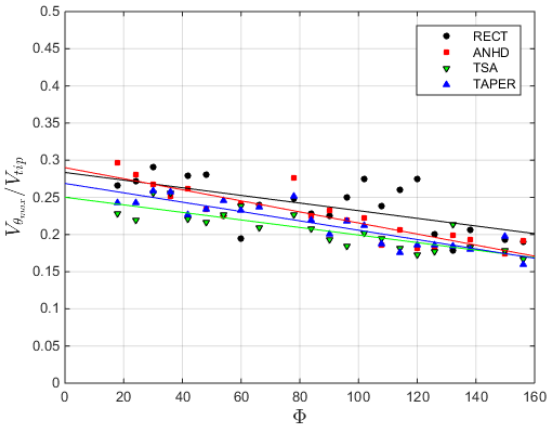

Figure 15: Maximum Tangential Velocities vs. Wake Age

Vortex meandering can be defined as random displacement of the vortex core. In Figure 16, scatter plots of the tip vortex centroids for a selection of phases are shown for the different cases. The amount of wander, as expected, increases with the increasing vortex age for all geometries. It can be seen that wandering motion is higher in axial coordinates and it rotates with increasing vortex age in a clockwise direction. It is also observed that in the TAPER and TSA configurations the wandering amplitude is greater than the other two cases.

The circulation of the tip vortex decreases as it convects downstream in the wake of the blades (see Figure 17). In accordance with the aerodynamic performance results, the circulation level in the case of the ANHD blade is the lowest. Apparently, the negative influence of the tip vortex on the aerodynamic performance of the blade in the sense of blade-vortex interaction is diminished in the case of the ANHD blade.

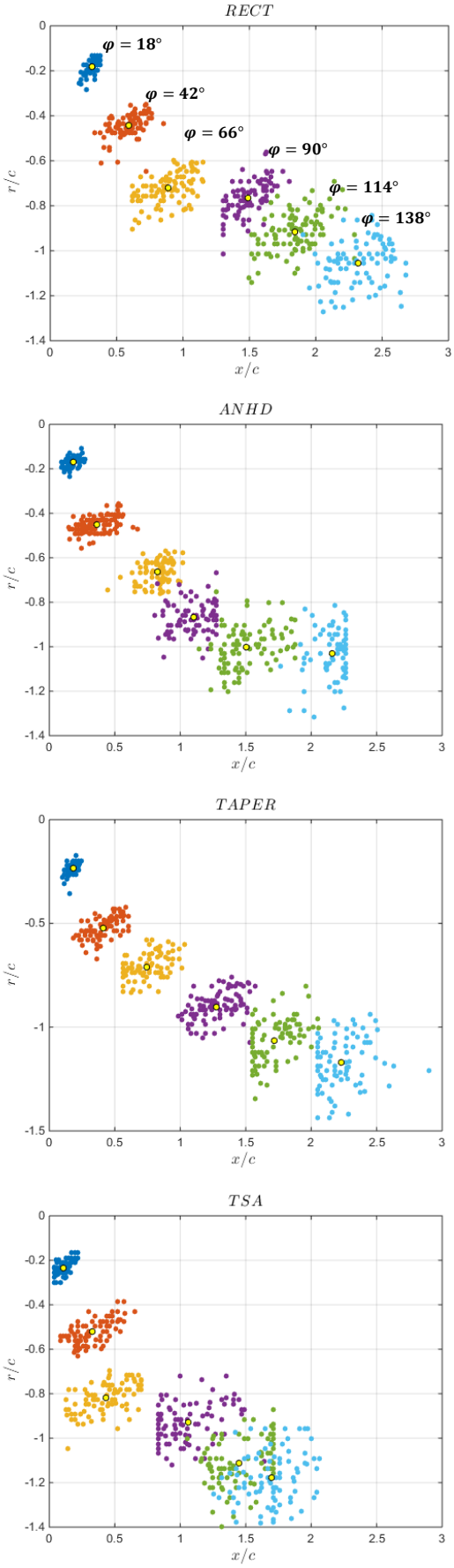

Figure 16: Scatter plots for $\varphi = 18°$ -138°

Presented at 44th European Rotorcraft Forum, Delft, The Netherlands, 19-20 September, 2018

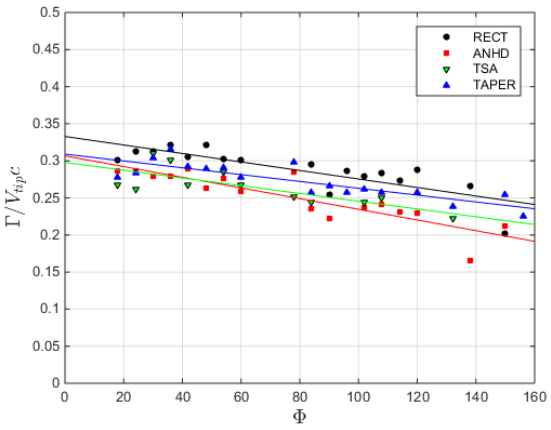

Figure 17: Tip Vortex Circulation vs. Wake Age

4. CONCLUSIONS

In this study, effects of different tip geometries on the aerodynamic performance and tip vortex characteristics of rotor blades are investigated experimentally. It was found that all tip modifications have a positive effect on the aerodynamic performance when compared to the rectangular tip configuration. This improvement is prominent especially at low blade loadings and the ANHD tip configuration gives the best performance at high blade loadings. Similarly, it was observed that tip modifications change vortex trajectory, reduce tangential velocity, and decrease the circulation levels of the tip vortex. The tip vortex shows a more stable behavior in the vicinity of the blade but the amplitude of the meandering increases as it convects downstream. The minimum tip-vortex circulation level is achieved in the case of the ANHD blade, which is in agreement with the highest figure of merit obtained with this blade.

ACKNOWLEDGEMENT

This study is part of a project supported by Turkish Aerospace Industries (TAI)-Rotary Wing Technology Center. The authors would like to thank Rotary Wing Technology Center and TAI-Helicopter group for their support and contribution.

COPYRIGHT STATEMENT

REFERENCES

[1] James L Tangler, Robert M. Wohlfeld, and Stan J Miley. An Experimental Investigation Of Vortex Stability, Tip Shapes, Compressibility, And Noise For Hovering Model Rotors, 1973.

[2] W. H. Weller. Experimental Investigation of Effects of Blade Tip Geometry on Loads and Performance for an Articulated Rotor System William, 1979.

[3] Baxter R Jr Mullins, Dudley E Smith, Curtis B Rath, and Sherry L Thomas. Helicopter Rotor Tip Shapes For Reduced Blade-Vortex Interaction - An Experimental Investigation, 1996.

[4] Preston B Martin, Moffett Field, and J Gordon Leishman. Trailing Vortex Measurements In The Wake of a Hovering Rotor Blade, 2002.

[5] Yong Oun J. Gordon Leishman Han. Investigation of Helicopter Rotor-Blade- Tip-Vortex, 2004.

[6] K. Kindler, K. Mulleners, H. Richard, B. G. Van Der Wall, and M. Raffel, Aperiodicity in the near field of full-scale rotor blade tip vortices,pp. 1601–1610, 2011.

[7] S. M. Mula, J. H. Stephenson, C. E. Tinney, and J. Sirohi, Dynamical characteristics of the tip vortex from a four-bladed rotor in hover, 2013.

[8] A. Bauknecht, B. Ewers, O. Schneider, and M. Raffel, Aerodynamic results from the STAR hover test: An examination of active twist actuation, *Proc. 41st Eur. Rotorcraft Forum*, 2015.

[9] M. R. C. Christian Wolf, Johannes N. Braukmann, Wolfgang Stauber, Till Schwermer, The Tip-Vortex System of a Four-Bladed Rotor in Dynamic Stall Conditions, *Ahs,* 2018.

[10] Graftieaux L, Michard M, Grosjean N. Combining PIV, POD and vortex identification algorithms for the study of unsteady turbulent swirling flows. *Meas. Sci. Technol. doi: 10.1088/0957-0233/12/9/307*, 2001.

[11] Keys, C. N., McVeigh, M. A., Dadone, L., and McHugh, F. J., Estimation of Full Scale Rotor Performance from Model Rotor Test Data, *Proceedings of the American Helicopter Society 39th Annual Forum*, 1983.

[12] J. G. Leishman, Principles of Helicopter Aerodynamics, 2nd Edition, Cambridge University Press, Cambridge, pp. 350-351, 2000.

[13] DTIC ADA033425: U.S. Army Helicopter Design Datcom Volume 1. Airfoils, 1976.

[14] D. Smith, D. Sigl, and D. E. Smith, Helicopter Rotor Tip Shapes for Reduced Blade Vortex Interaction an Experimental Investigation, *The University of Oklahoma Norman , OK 33rd Aerospace Sciences Meeting and Exhibit,* 1995.

Presented at 44th European Rotorcraft Forum, Delft, The Netherlands, 19-20 September, 2018